HOKKAIDO UNIVERSITY

Title	FE MODELING OF THE PEEL BEHAVIOR OF EXTERNALLY BONDED FRP REINFORCEMENT FROM A CONCRETE SUBSTRATE
Author(s)	DAI, J. G.; BAI, Y. L.; TENG, J. G. et al.
Description	The Thirteenth East Asia-Pacific Conference on Structural Engineering and Construction (EASEC-13), September 11-13, 2013, Sapporo, Japan.
Relation	Proceedings of the Thirteenth East Asia-Pacific Conference on Structural Engineering and Construction (EASEC-13), September 11-13, 2013, Sapporo, Japan, G-5-1.
Citation	Proceedings of the Thirteenth East Asia-Pacific Conference on Structural Engineering and Construction (EASEC-13), G-5-1
Issue Date	2013-09-13
Doc URL	https://hdl.handle.net/2115/54431
Type	conference paper
File Information	easec13-G-5-1.pdf

Hokkaido University Collection of Scholarly and Academic Papers

Hokkaido University Collection of Scholarly and Academic Papers : HUSCAP

FE MODELING OF THE PEEL BEHAVIOR OF EXTERNALLY BONDED FRP REINFORCEMENT FROM A CONCRETE SUBSTRATE

J.G. DAI[1*†], Y.L. BAI[1], J.G. TENG[1], L.DE LORENZIS[2] and W.Y. GAO[1]

[1]*The Hong Kong Polytechnic University, Hong Kong, China*
[2]*Technische Universität,, Germany*

ABSTRACT

This paper presents a finite element (FE) study into the peel behavior of FRP reinforcement externally bonded to a concrete substrate where the peel force leads to a mixed-mode loading condition for the FRP-to-concrete interface. A mixed-mode cohesive zone model is employed in the FE model to represent the interaction between Mode I and Mode II loading actions. The focus of the FE study is on the full-range mixed-mode debonding behavior of the-FRP-to-concrete interface (i.e. covering both an unstable debonding stage and a steady debonding stage). The FE results allow the effects of various geometric, material and loading parameters to be examined in the paper, where particular attention is paid to the effect of the peel (loading) angle. It is shown that the mechanism of interaction between Mode I and Mode II varies with the peel angle and the Mode I component has a significant effect on the interfacial debonding process even when the peel angle is small.
Keywords: FRP-to-concrete interface, mixed-mode loading, debonding, peel test.

1. INTRODUCTION

In concrete members strengthened with externally bonded fiber reinforced polymer (FRP) composites, debonding of FRP-to-concrete interfaces usually is a dominant failure mode particularly in bond-critical applications (i.e. flexural and shear strengthening). A good understanding has been achieved on the various debonding failure modes in FRP-strengthened reinforced concrete (RC) beams (e.g. Teng et al. 2002). These failure modes were usually defined based on the failure mechanisms/appearances of FRP-strengthened RC members. According to the stress conditions to which FRP-to-concrete interfaces are exposed, the debonding failure in fact can be simply classified into three categories: mode I, mode II and mixed-mode failure (e.g. Ueda and Dai 2005), which correspond to an FRP bonded to a concrete substrate subjected to a pull action (i.e. parallel to the FRP plane), a peel action (i.e. perpendicular to the FRP plane) and a combined peel and pull action, respectively.

Recently, increasing work has been conducted both experimentally and analytically on the mixed-mode failure of FRP-to-concrete interfaces (e.g. Wan et al. 2004; Yao et al. 2005; Wu et al. 2005; Dai et al. 2007; Pan and Leung 2007). The analytical work has been based upon either closed-form solutions (e.g. Wang 2007; Pan and Leung 2007; De Lorenzis and Zavarise 2008; Dai

* Corresponding author: Email: cejgdai@polyu.edu.hk

† Presenter: Email: cejgdai@polyu.edu.hk

et al. 2009) or finite element (FE) analyses (e.g. Kishi et al. 2005; Niu et al. 2006; De Lorenzis and Zavarise 2008; Lee et al. 2010; Tayyebeh et al. 2010). However, two major issues still remain controversial on the debonding failure of FRP-to-concrete interfaces subject to mixed-mode loading. The first issue is the quantitative relationship between the peel angle, which is the angle between the peeled FRP and the concrete substrate, and the mode II debonding strength of FRP particularly when the peel angle is small (i.e. usually the situation in FRP flexurally-strengthened RC members). The second issue is the identification of the most suitable normal separation and tangential traction laws for FRP-to-concrete interfaces subject to a mixed-mode loading condition. The objective of the present paper is to further understand the above-mentioned two issues through a careful FE analysis of a typical peel test for the FRP-to-concrete interface.

2. PEEL TEST AND LINEAR ELASTIC FRACTURE MECHANICS (LEFM) ANALYSIS

The peel test is a conventional test method for which a thin film is bonded to a substrate and pulled from it at a certain angle (referred to as "peel angle") as shown in Fig.1. As a result the interface is subjected to both normal and shear stresses, leading to a mixed-mode interface fracture condition. For the particular case of the FRP-concrete interface, previous studies have shown as a large peel angle corresponds to a dominant mode I fracture and a small peel angle is involved with a high degree of mode mixity (De Lorenzis and Zavarise 2008). Based upon the linear elastic fracture mechanics (LEFM) assumption, the mode I and mode II energy release rates, G_I and G_{II}, during the mixed-mode debonding of FRP-to-concrete interfaces in a peel test can be calculated as follows (Thouless and Jensen 1992):

$$G_I = \frac{6M_0^2}{Et^3} \qquad G_{II} = \frac{F_0^2}{2Et} \tag{1}$$

$$M_0 = \sqrt{\left[\frac{Et^3}{6}\cdot\frac{F_{peel}{}^2\sin^2\theta}{2Et} + F_{peel}(1-\cos\theta)\right]}; \quad F_0 = F_{peel}\cos\theta \tag{2}$$

where F_0, M_0 are the mode II force component and the moment in the FRP at the tip of the interface crack (Fig.1), respectively; F_{peel} is the peel force (Fig.1); E is the elastic modulus of FRP; t is the thickness of FRP; and θ is the peel angle between the FRP and the concrete substrate.

The mixed-mode fracture propagation of FRP-to-concrete interfaces is governed by a fracture energy-based failure envelope. Two typical types of failure criteria have been adopted by previous researchers for FRP-to-concrete interfaces subjected to mixed-mode loading (De Lorenzis and Zavarise 2008; Lee et al. 2010) as follows:

$$G_I / G_{1f} + G_{II} / G_{2f} = 1 \tag{3}$$

$$\left(\frac{G_I}{G_{1f}}\right)^2 + \left(\frac{G_{II}}{G_{2f}}\right)^2 = 1 \tag{4}$$

where G_{1f} and G_{2f} are the interfacial fracture energies under pure mode I and mode II conditions, respectively. With a combined use of Eqs.1 to 4, the relationship between the peel

force and the peel angle can be obtained without difficulties, see De Lorenzis and Zavarise (2008) for all details.

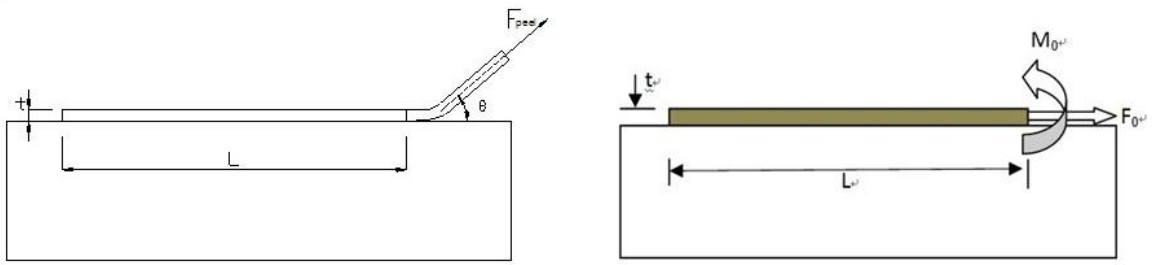

Figure 1: Schematic of a peel test.

3. FINITE ELEMENT MODELING OF THE PEEL TEST

The closed-form solutions presented above can only be used to predict the steady state peel force of the FRP-to-concrete interface as explained later. In addition, the nonlinearity of FRP-to-concrete interfaces, which has been proven to be very significant particularly when the mode II loading effect is predominant, cannot be appropriately considered in such analyses. Therefore, a 2-dimensional (2D) FE model is deployed in the present paper to simulate the peel test thereby overcoming the limitations of the closed-form solutions. In the FE model, the FRP is modeled using plane stress elements and as an orthotropic material whereas the substrate concrete is treated as a rigid body. Cohesive interface elements are incorporated along the nodes between the FRP and the concrete at the same geometric locations.

A bilinear model is used to describe the cohesive behavior of the FRP-to-concrete interface in both normal and tangential directions (Fig.2). Two different criteria are used to evaluate the debonding initiation of the FRP-to-concrete interface. One is to assume that the mode I and mode II debonding initiations are independent from each other (De Lorenzis and Zavarise 2008). As a result, the debonding initiation law (DIL) of the FRP-to-concrete interface can be expressed as:

$$\max\left\{\frac{\sigma_n}{\sigma_n^0},\frac{\tau_n}{\tau_s^0}\right\}=1 \tag{5}$$

where σ_n and τ_n are the peak normal stress and shear stress at the interface at the initiation of the mixed-mode debonding, respectively; σ_n^0 and τ_s^0 are the peak normal stress and shear stress at the interface at the debonding initiation of the interface under a single mode I and mode II loading, respectively. The other is to assume that the normal and shear stresses have coupled effects and the mixed-mode interface debonding will initiate when the following stress condition is reached:

$$\left(\frac{\sigma_n}{\sigma_n^0}\right)^2+\left(\frac{\tau_s}{\tau_s^0}\right)^2=1 \tag{6}$$

Similarly, two different types of debonding propagation law (DPL) (i.e. Eq.3 and Eq.4) are used in the FE analysis for comparative purposes.

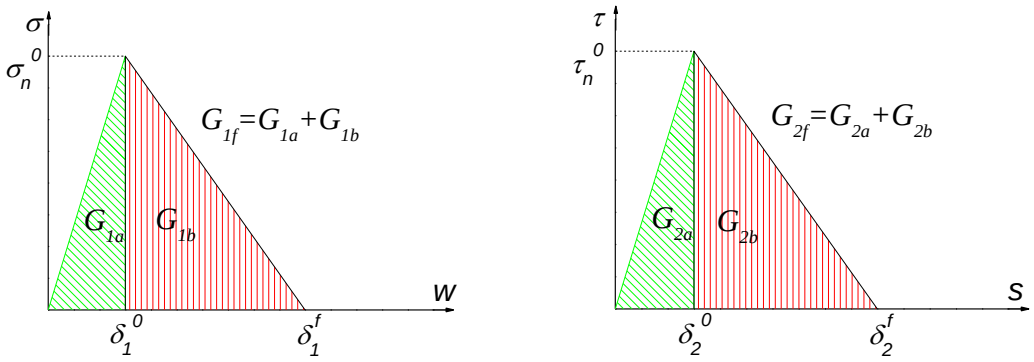

(a) Traction law in normal direction (mode I) (b) Traction law in tangential direction (mode II)

Figure 2: Cohesive zone models for Mode I and Mode II interface debonding.

4. FE ANALYTICAL RESULTS

As the first step, the FRP-to-concrete interface is assumed to be linear elastic in both normal and tangential directions to validate the FE model through comparisons with the LEFM based closed-form solutions as discussed in **Section 2**. In other words, both the normal and tangential traction laws are assumed to be of linear brittle type. Major parameters used for the analysis are given the following values: G_{1f} = 0.1N/mm; G_{2f} = 0.4N/mm; σ_n^0=2MPa; and τ_s^0 = 4MPa. Only Eq. 3 is applied to govern the debonding propagation of the FRP-to-concrete interface. Other details about the analysis can be found in Dai et al. (2013). Fig.3 presents the peel force vs. displacement relationships at the loaded ends of FRP in cases of different peel angles. It is shown that the load-displacement response generally consists of two significant stages: an ascending branch up to the first peak peeling load and a flat branch. The constant peel force maintained at the latter stage is denoted as the steady state debonding load. A descending branch may exist after the first peak peeling load if the peel angle is relatively large (e.g. 4^0, Fig.3). It is also shown that the steady state debonding load decreases with the increase of peel angle (Fig.4). When the peel angle increases from 0 to 4^0, the steady state peeling load decreases down to about one quarter of the pure mode II debonding load (i.e. the peel angle is 0^0). The closed-form solutions on the steady-state peeling loads at different peel angles are also given in Fig.4. Two other lines obtained by assuming that Eq.3 is replaced by $G=G_I+G_{II}=G_{1f}$ *or* $G=G_I+G_{II}=G_{2f}$ are provided as well in Fig.4 for references. It is seen that the FE analytical and the closed-form solutions lead to consistent prediction of the steady state peeling loads for all the peel angles. It is also seen that, when the peel angle increases to 4^0, both the FE prediction and the closed-form prediction all approach the curve obtained by assuming $G=G_{1f}$, indicating that the debonding failure of FRP-to-concrete interfaces is mode I dominant.

Results from the above FE analyses and closed-form solutions provide useful information for understanding the change of the mode-mixity and the steady state peeling load with the peel angle. However, they do not provide an insightful investigation into the mixed-mode debonding mechanisms of the FRP-to-concrete interfaces under different peel angles due to the limitations of the LEFM-based assumption. Therefore, further numerical experimentations were conducted to investigate effects of various geometric, material and loading parameters on the full-range debonding behavior of the FRP-to-concrete interfaces. Two typical peel angles were chosen for the

numerical experimentations: one is 2^0 and the other is 8^0, representing typical small and large peel angles, respectively.

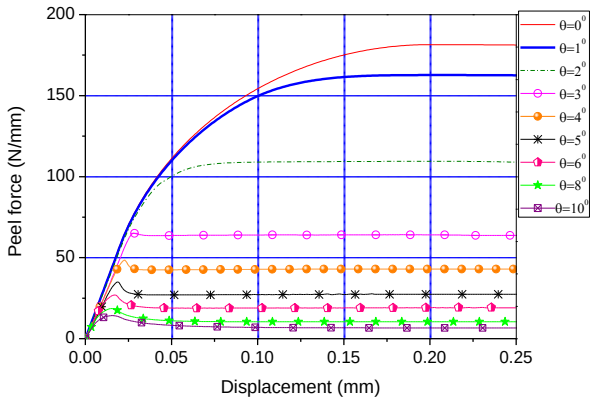

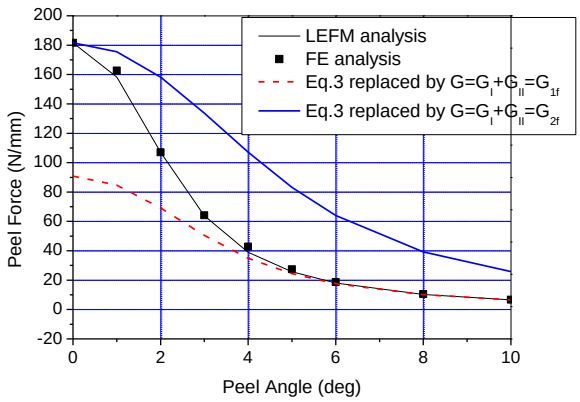

Figure 3: Peeling load vs. displacement. **Figure 4: Steady state peeling load vs peel angle.**

For the LEFM analyses, once the properties of the FRP (i.e. the elastic modulus E and the thickness of t), the mode I and mode II interfacial fracture energies (i.e. G_{1f}, G_{2f}) and the debonding propagation law (i.e. Eq.3 or Eq.4) are given, the steady state peel load of the FRP-to-concrete interface can be determined. However, besides the interfacial fracture energies, there are many other parameters influencing the configuration of the mixed-mode cohesive zone models and consequently the full-range debonding behavior of the FRP-to-concrete interface subjected to mixed-mode loading. To investigate the effects of these parameters, the bilinear traction law of the FRP-to-concrete interface in the normal direction is described with two parts (Fig.2): an ascending part and a descending part. The areas underneath these two parts are respectively denoted as G_{1a} and G_{1b}. The crack openings of the interface corresponding to the peak local normal stress and the free local normal stress are denoted as δ_1^0 and δ_1^f, respectively. Similar denotations are applied for the tangential direction of the FRP-to-concrete interfaces while the corresponding symbols are denoted as G_{2a}, G_{2b}, δ_2^0 and δ_2^f, respectively. Given the value of G_{1f} (G_{2f}), the shape of the normal (tangential) traction law of the FRP-to-concrete interface can be determined with the value of σ_n^0 (τ_s^0) and the ratio of G_{1a} to G_{1b} (G_{2a} to G_{2b}). A larger ratio means a more significant nonlinearity of the interface.

Figs.5a and 5b present the effects of the shape of the cohesive zone models on the steady state peel loads. In these parametric analyses, only the two-node beam elements are used for simulating the FRP and the DPL and DIL are described with Eqs.3 and 5, respectively. In these figures, only the effects of the configuration of the mode I traction law on the peel force are presented for simplicity while the tangential traction law is fixed (i.e. G_{2a}/G_{2b} = 1:9 and τ_s^0 = 4MPa), since the effects of the configuration of mode I and mode II traction laws are believed to be similar due to their similar shape. Analytical results show that the peak normal stress just has a slight influence (Fig.5a) while the ratio of G_{1a} to G_{1b} has influences significantly the steady state peel load (Fig.5b). When such a ratio is 1:9, the FE prediction based upon the cohesive zone models (i.e. an NLFM approach) deviates significantly from the LEFM approach prediction and the FE prediction tends to approach the curve obtained by assuming $G=G_{2f}$ (Fig.5a) when the peel angle is small. In other words, the

interface tends to shift to a mode II dominant debonding failure. If the ratio of G_{1a} to G_{1b} increases from 1:9 to 2:3, that is, the proportion of the elastic fracture energy consumed during the debonding increases, the FE prediction on the steady state peel load almost coincides with the closed-form solution prediction based on the LEFM.

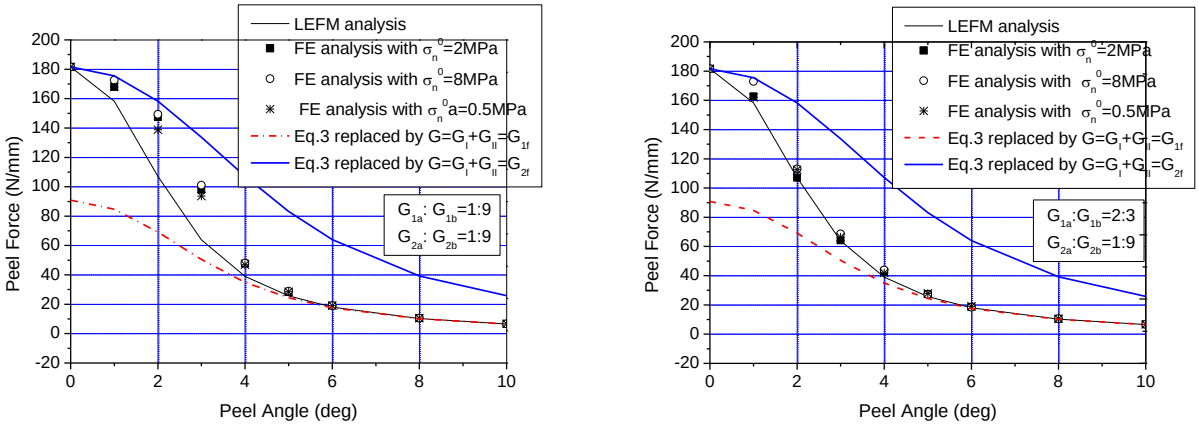

(a) effect of the peak normal stress (b) effect of the ratio of the ratio of G_{1a} to G_{1b}

Figure 5: Effects of the cohesive zone behavior on the steady state peel loads

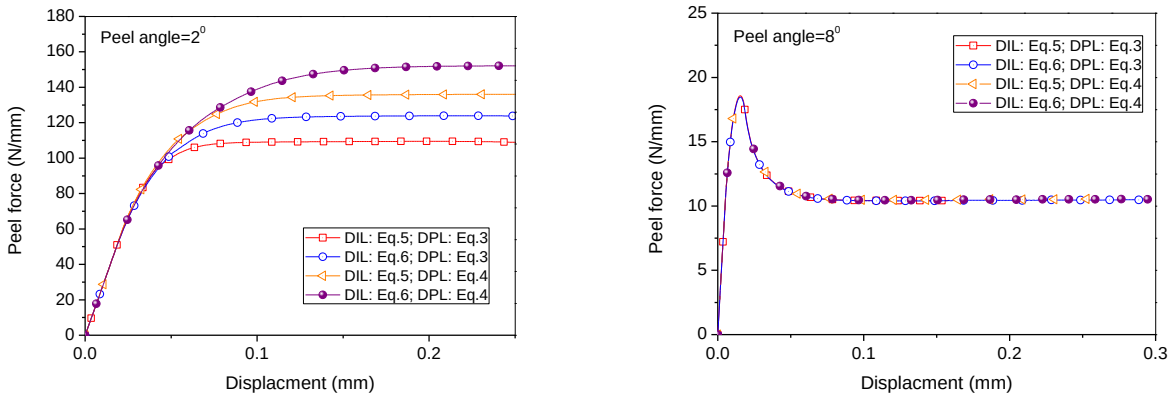

(a) small peel angle (b) large peel angle

Figure 6: Coupled effects of mode I/mode II loading on the peel load-displacement response

To further understand the coupled effects of the mode I and mode II loadings on the debonding of FRP-to-concrete interfaces, parametric analyses were also conducted based upon the FE model using two different DILs (Eqs.5 and 6) and DPLs (Eqs.3 and 4). The analytical results are presented in Figs.6a and 6b, in which the peel force vs. displacement relationships are given for a small peel angle and a large peel angle, respectively. It is shown that with a small peel angle (i.e. 2^0), both the DIL and the DPL influence significantly the steady state debonding load However, for a large peel angle, both the DIL and DPL just have marginal effects on the initial peel and steady state peel loads. For a small peel angle, if the interfacial fracture energies G_{1f} and G_{2f} are kept the same, the use of Eq.5 as the DPL or Eq.4 as the DIL leads to a conservative prediction of the steady state debonding load. Figures 7a and 7b present the analytical results on the effects of G_{1f} and G_{2f} on the peel force vs. displacement relationships. Given a small peel angle, both the first peak peel load and

the steady state peel load increase with the G_{1f} and G_{2f} (Fig.7a). However, in case of a large peel angle, only G_{1f} influences the first peak peel load and the steady state peel load, while G_{2f} only has very little influence on them (Fig.7b). These analytical results have further demonstrated that the debonding of FRP-to-concrete interface has completely become mode I dominant once the peel angle reaches a relatively large value (e.g. 8^0).

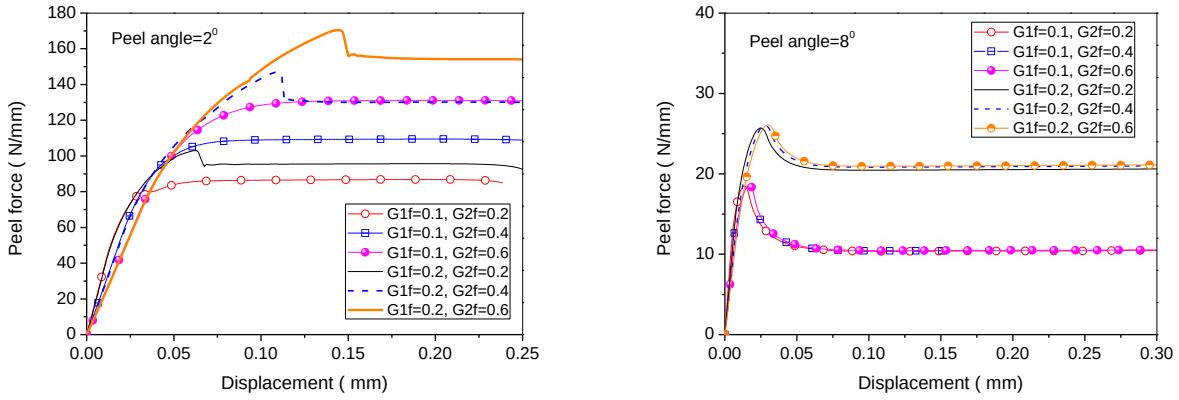

(a) small peel angle (b) large peel angle

Figure 7: Effects of G_{1f} and G_{2f} on the peel load-displacement response

5. CONCLUSIONS

This paper has conducted a finite element study on the mixed-mode bond behavior of FRP-to-concrete interfaces subjected to peel force. Extensive parametric studies have been conducted for FRP-to-concrete interfaces with two peel angles, 2^0 and 8^0, representing a typical small peel angle and a typical large peel angle, respectively. The following conclusions can be drawn according to the analytical results:

1. The peel force decreases significantly with the increase of the peel angle. Once the peel angle increases from 0^0 to 4^0, the debonding failure of FRP-to-concrete interfaces has shifted from a pure mode II failure to a mode I dominant failure. A high degree of mode mixity exists in the FRP-to-concrete interface at a small peel angle, under which circumstance the mode I component has a significant effect on the mode II debonding strength of FRP.
2. The peel force vs. displacement relationship of FRP-to-concrete interface under mixed-mode loading usually has a first ascending branch, followed by a descending and then a steady-state branch.
3. Given a small peel angle, when the mode I/mode II interfacial fracture energy is kept constant, the peak normal/shear stress in the mode I separation/mode II traction law influences slightly the steady state peel load. Instead, the ratio of the mode I fracture energy consumed at the elastic stage to that consumed at the softening stage influences greatly the steady state peel load. At a large peel angle, the mode I/mode II interfacial fracture energy is the only influential parameter.
4. For a small peel angle, the prediction of the peel load largely depends on the configuration of the mixed-mode cohesive zone model, in terms of both the debonding initiation criterion and the debonding propagation criterion. The coupled effects of mode I and mode II loadings on these

two criteria influence significantly the prediction of the whole range debonding behaviour of the FRP-to-concrete interface. However, for a large peel angle, it is no longer important to consider such coupled effects and the initial peak and steady-state peel loads just increase with the mode I interfacial fracture energy.

6. ACKNOWLEDGMENTS

The authors are grateful for the financial support received from the Research Grants Council of the Hong Kong SAR (Project No: PolyU516509).

7. REFERENCES

Dai, J.G., Ueda, T. and Sato, Y. 2007. Bonding characteristics of fiber-reinforced polymer sheet-concrete interfaces under dowel load. Journal of Composites for Construction, ASCE, 11(2), 138-148.

Dai, J.G., Wan, B., Yokota, H. and Ueda, T. 2009. Fracture criterion for carbon fiber reinforced polymer sheet to concrete interface subjected to coupled pull-out and push-off actions. Advances in Structural Engineering, 12(5), 663-682.

Dai, J.G., Bai Y.L., Teng, J.G., De Lorenzis, L., Gao W. Y. 2013. Modeling the Debonding of FRP-to-Concrete Interfaces Subjected to Mixed-Mode Loading. In preparation.

De Lorenzis, L. and Zavarise, G. 2008. Modeling of mixed-mode debonding in the peel test applied to superficial reinforcements. International Journal of Solids and Structures, 45(20), 5419-5436.

Kishi, N., Zhang, G. F. and Mikami, H. 2005. Numerical cracking and debonding analysis of RC beams reinforced with FRP sheet. Journal of Composites for Construction, ASCE, 9(6), 507-514.

Lee, J. H., Chacko, R. M. and Lopez, M. M. 2010. Use of mixed-mode fracture interfaces for the modeling of large-scale FRP-strengthened beams. Journal of Composites for Construction, ASCE, 14(6), 845-855.

Niu, H., Karbhari, V. M. and Wu, Z. 2006. Diagonal macro-crack induced debonding mechanisms in FRP rehabilitated concrete. Composites Part B: Engineering, 37(7-8), 627-641.

Pan, J. and Leung, C. K. Y. 2007. Debonding along the FRP-concrete interface under combined pulling/peeling effects. Engineering Fracture Mechanics, 74(1-2), 132-150.

Tayyebeh Mohammadi, B. Wan and J.G. Dai. 2011. Modeling of CFRP-concrete interface subjected to coupled pull-out and push-off actions. ACI Special Publication. 275, 1-18.

Teng, J. G., Chen, J. F, S. T. Smith and L. Lam. 2002. FRP-strengthened RC structures. Chichester, England, Wiley.

Thouless, M.D., Jensen, H.M., 1992. Elastic fracture mechanics of the peel-test geometry. Journal of Adhesion, 38, 185–197.

Ueda T and Dai J.G. 2005. Interface bond between FRP sheets and concrete substrates: numerical modelling and roles in member behaviour, Progress in Structural Engineering and Materials, 7(1), 27-43.

Wan, B. L., Sutton, M. A., Petrou, M. F., Harries, K. and Ning, U. 2004. Investigation of bond between fiber reinforced polymer and concrete undergoing global mixed mode I/II loading. Journal of Engineering Mechanics, ASCE, 130(12), 1467-1475.

Wu, Z. S., Yuan, H., Asakura, T., Yoshizawa, H., Kobayashi, A. and Kojima, Y. 2005. Peeling behavior and spalling resistance of bonded bidirectional fiber reinforced polymer sheets. Journal of Composites for Construction, ASCE, 9(3), 214-226.

Wang, J. 2007. Cohesive zone model of FRP-concrete interface debonding under mixed-mode loading. International Journal of Solids and Structures, 44(20), 6551-6568.

Yao, J., Teng, J. G. and Chen, J. F. 2005. Experimental study on FRP-to-concrete bonded joints. Composites Part B: Engineering, 36(2), 99-113.